

University of Wollongong

Research Online

Australian Institute for Innovative Materials -
Papers

Australian Institute for Innovative Materials

1-1-2012

Strain modulated transient photostriction in La and Nb codoped multiferroic BiFeO₃ thin films

Zuanming Jin
Shanghai University

Yue Xu
Shanghai University

Zhengbing Zhang
Shanghai University

Xian Lin
Shanghai University

Guohong Ma
Shanghai University

See next page for additional authors

Follow this and additional works at: <https://ro.uow.edu.au/aiimpapers>



Part of the [Engineering Commons](#), and the [Physical Sciences and Mathematics Commons](#)

Research Online is the open access institutional repository for the University of Wollongong. For further information contact the UOW Library: research-pubs@uow.edu.au

Strain modulated transient photostriction in La and Nb codoped multiferroic BiFeO₃ thin films

Abstract

The coherent longitudinal acoustic (LA) phonons in La and Nb codoped polycrystalline BiFeO₃ (Bi_{0.8}La_{0.2}Fe_{0.99}Nb_{0.01}O₃ (BLFNO)) films are photo-induced and detected by the ultrafast reflectance spectroscopy. The generation mechanism of LA phonons is strongly connected with the ferroelectric polarization and is attributed to the transient photostriction effect, which is a combination of the optical rectification effect and the electrostriction effect. The strain modulation of sound velocity and out-of-plane elastic properties are demonstrated in BLFNO film on SrTiO₃, which gives the insight on the dynamical coupling between electrical polarization and lattice deformation. Our findings are desired for the design of BiFeO₃-based photo-driven remote control micro/nano devices. 2012 American Institute of Physics.

Keywords

nb, films, la, multiferroic, photostriction, bifeo3, transient, modulated, codoped, strain, thin

Disciplines

Engineering | Physical Sciences and Mathematics

Publication Details

Jin, Z., Xu, Y., Zhang, Z., Lin, X., Ma, G., Cheng, Z. & Wang, X. (2012). Strain modulated transient photostriction in La and Nb codoped multiferroic BiFeO₃ thin films. *Applied Physics Letters*, 101 (24), 242902-1-242902-5.

Authors

Zuanming Jin, Yue Xu, Zhengbing Zhang, Xian Lin, Guohong Ma, Zhenxiang Cheng, and Xiaolin Wang

Strain modulated transient photostriction in La and Nb codoped multiferroic BiFeO₃ thin films

Zuanming Jin, Yue Xu, Zhengbing Zhang, Xian Lin, Guohong Ma et al.

Citation: *Appl. Phys. Lett.* **101**, 242902 (2012); doi: 10.1063/1.4770309

View online: <http://dx.doi.org/10.1063/1.4770309>

View Table of Contents: <http://apl.aip.org/resource/1/APPLAB/v101/i24>

Published by the American Institute of Physics.

Related Articles

Polarization reversal and dynamic scaling of (Na_{0.5}K_{0.5})NbO₃ lead-free ferroelectric ceramics with double hysteresis-like loops

J. Appl. Phys. **112**, 104114 (2012)

Dislocation-induced fields in piezoelectric AlGaN/GaN bimaterial heterostructures

J. Appl. Phys. **112**, 103501 (2012)

Excellent dielectric properties of anisotropic polymer composites filled with parallel aligned zinc flakes

Appl. Phys. Lett. **101**, 192904 (2012)

Conductivity in disordered structures: Verification of the generalized Jonscher's law on experimental data

J. Appl. Phys. **112**, 094107 (2012)

Positive effective Q₁₂ electrostrictive coefficient in perovskites

J. Appl. Phys. **112**, 094106 (2012)

Additional information on *Appl. Phys. Lett.*

Journal Homepage: <http://apl.aip.org/>

Journal Information: http://apl.aip.org/about/about_the_journal

Top downloads: http://apl.aip.org/features/most_downloaded

Information for Authors: <http://apl.aip.org/authors>

ADVERTISEMENT

AIP | Applied Physics
Letters

1µm-thick LPCVD Silicon Dioxide, Ground Ring, Drain, Metal Vias

SURFACES AND INTERFACES
Focusing on physical, chemical, biological, structural, optical, magnetic and electrical properties of surfaces and interfaces, and more...

EXPLORE WHAT'S NEW IN APL
SUBMIT YOUR PAPER NOW!

ENERGY CONVERSION AND STORAGE
Focusing on all aspects of static and dynamic energy conversion, energy storage, photovoltaics, solar fuels, batteries, capacitors, thermoelectrics, and more...

Strain modulated transient photostriction in La and Nb codoped multiferroic BiFeO₃ thin films

Zuanming Jin,¹ Yue Xu,¹ Zhengbing Zhang,¹ Xian Lin,¹ Guohong Ma,^{1,a)} Zhenxiang Cheng,^{2,b)} and Xiaolin Wang²

¹Laboratory of Ultrafast Photonics, Department of Physics, Shanghai University, 99 Shangda Road, Shanghai 200444, People's Republic of China

²Institute for Superconductor and Electronic Materials, University of Wollongong, Squires Way, North Wollongong, NSW 2500, Australia

(Received 26 August 2012; accepted 26 November 2012; published online 10 December 2012)

The coherent longitudinal acoustic (LA) phonons in La and Nb codoped polycrystalline BiFeO₃ (Bi_{0.8}La_{0.2}Fe_{0.99}Nb_{0.01}O₃ (BLFNO)) films are photo-induced and detected by the ultrafast reflectance spectroscopy. The generation mechanism of LA phonons is strongly connected with the ferroelectric polarization and is attributed to the transient photostriction effect, which is a combination of the optical rectification effect and the electrostriction effect. The strain modulation of sound velocity and out-of-plane elastic properties are demonstrated in BLFNO film on SrTiO₃, which gives the insight on the dynamical coupling between electrical polarization and lattice deformation. Our findings are desired for the design of BiFeO₃-based photo-driven remote control micro/nano devices. © 2012 American Institute of Physics. [<http://dx.doi.org/10.1063/1.4770309>]

Multiferroics are materials that exhibit simultaneous coexistence of electric and magnetic orders parameters. Bismuth ferrite BiFeO₃ (BFO) is identified as a classical single-phase magnetoelectric multiferroic at room temperature so far, which shows high-temperature ferroelectricity (Curie temperature $T_c \sim 1100$ K) with a large electric polarization of above $100 \mu\text{C}/\text{cm}^2$. Bulk crystalline BFO adopts incommensurate magnetic order in a G-type antiferromagnetic state below Néel temperature $T_N \sim 640$ K with a cycloidal spin arrangement with a long modulation period of $\lambda \approx 620 \text{ \AA}$.¹⁻³ Both control of magnetization with electric fields and modification of electric polarization with magnetic fields would lead to a variety of potential applications in optoelectronics and spintronic devices.^{4,5}

In recent years, more and more attention have been focused on the linear,^{6,7} nonlinear optical properties,^{8,9} and the photo-induced effects in multiferroic BFO.¹⁰⁻¹⁵ Noteworthy, photo-induced effects can be coupled to functional properties, such as ferroelectricity, ferromagnetism, and ferroelasticity of BFO. For example, when illuminated by ultraviolet light in an open circuit, the magnitude of the photovoltage was found to be proportional to the crystal length along the electric polarization direction.^{12,13} Rana *et al.* reported that the ultrafast depolarization of ferroelectric order causes the structural dependent terahertz radiation in BFO.¹⁶ Talbayev *et al.* used the terahertz spectroscopy to interpret the spectrum of long-wavelength magnetic resonance modes of BFO crystal.¹⁷ Coupling of light with mechanical degrees of freedom in BFO was reported by Kundys *et al.*, the light-induced wavelength dependent size change of BFO single crystal can be understood from photostriction effect, a superposition of photovoltaic effect and electrostrictive effect.^{14,15} Although the photostriction effect has been found in BFO single crystal at room temperature, it remains

intensive investigation aiming to understand the dynamical photostriction effect. We would like to mention that the La and Nb codoped BFO film shows a much higher electrical polarization than that of intrinsic BFO film,¹⁸ and therefore the enhanced photostriction effect in doped BFO is expected. However, there are few experimental reports about the transient photostriction effect modified by the doping effect and the strain effect introduced by substrate. Ultrafast spectroscopy is employed as an efficient tool to investigate the dynamical properties due to its ability to simultaneously probe the evolution of multiple degrees of freedom in the time domain.¹⁹ In this letter, all optical pump-probe technique was employed to investigate the transient photostriction effect in La and Nb codoped multiferroic Bi_{0.8}La_{0.2}Fe_{0.99}Nb_{0.01}O₃ (BLFNO) thin films on different substrates. The observed low frequency coherent longitudinal acoustic (LA) phonons in BFO film is originated from the polarization induced by optical rectification, which is efficiently enhanced by La and Nb codoped. In addition, the out-of-plane elastic constant of BLFNO film is strongly modulated by the strain effect in epitaxially grown BLFNO film on SrTiO₃.

The thin film samples in this work were deposited using a pulsed laser deposition system. Third harmonic generation of a Nd doped yttrium aluminum garnet laser with a wavelength of 355 nm and a repetition rate of 10 Hz was used as the laser source. BLFNO thin films were deposited on p-type (001)-Si, yttrium stabilized (001)-ZrO₂ (YSZ), and (001)-SrTiO₃ (STO) at 550 °C, then cooled down to room temperature following rapid thermal processing. During the deposition, the dynamic oxygen flow pressure was kept at 20 mTorr. The BLFNO film on (001)-STO is epitaxially grown with tetragonal structure, which is evidenced by X-ray diffraction. The film thickness is about 200 nm. Details of the samples have been reported elsewhere in Ref. 20.

The transient reflectivity changes reported here are performed using a dual-color pump-probe technique. The light source is provided by a commercial mode-locked Ti:sapphire

^{a)}Email address: ghma@staff.shu.edu.cn.

^{b)}Email address: cheng@uow.edu.au.

laser (Spitfire Pro, Spectra-Physics) operated at a repetition rate of 1 kHz, the pulse width of 120 fs, and the center wavelength of 800 nm. The output pulse train is split by a beam splitter. After the beam splitter, the major part is frequency-doubled in a 1-mm BBO crystal as the pump beam of $\sim 0.8 \text{ mJ/cm}^2$ at the center wavelength of 400 nm (above the E_g of BFO), and the other part without doubling (below the E_g of BFO) is as the probe beam of $\sim 0.08 \text{ mJ/cm}^2$. The pump beam is modulated at 490 Hz with a mechanical chopper. Both of the pump and probe beams are focused on the surface of samples with near normal incidence. The reflected probe beam is detected by a photodiode connected with a lock-in amplifier to enhance the signal to noise ratio. The sample is mounted on a cold finger in a closed cycle liquid-He cooled optical cryostat with four transparent windows.

Figure 1(a) presents a schematic of the pump-probe technique and photo-induced LA phonon propagation configuration. BFO contains transition metal ions with unpaired 3d electrons, which results in a relatively small optical gap ($E_g \sim 2.6\text{--}2.8 \text{ eV}$) in contrast to other conventional ferroelectric perovskites at room temperature.⁶ Thus, as the photo-energy of the pump pulse ($E_{\text{pump}} = 3.1 \text{ eV}$) is larger than the optical gap of the BFO, the electron-hole pairs are generated.^{12,15} In addition, for a material with non-centrosymmetry, the second-order polarization $P^{(2)}(t)$ can be described by^{21,22}

$$P^{(2)}(t) = \epsilon_0 \chi^{(2)} E(t) E^*(t) = P_0^{(2)}(t) + P_{2\omega}^{(2)}(t), \quad (1)$$

where $\chi^{(2)}$ is the nonlinear susceptibility. $E(t)$ and $E^*(t)$ are the optical electric field and its conjugate, respectively. The first term on the right side of Eq. (1) is the optically induced polarization to acquire a dc term, i.e., the optical rectification effect, and the second term is associated with the second harmonic generation.⁸ Through the electrostriction effect, the dc term of the second-order polarization $P_0^{(2)}(t)$ leads to a significant lattice deformation and then emits LA phonons.²²

The LA phonons excited by pump beam will create a strain wave in the BFO film. As this strain wave propagates through the sample, the probe pulse undergoes a Doppler shift following the interaction with the moving strain wave, as in stimulated Brillouin scattering. The propagation of the LA phonons can be recorded by scanning the time delay between the pump and probe pulses.

Figures 1(b) and 1(d) show the typical transient reflectivity changes ($\Delta R/R$) of BLFNO thin films on (001)-STO and (001)-Si substrate, respectively. $\Delta R/R$ consists of a swift rise followed by fast-, slow-relaxation, and oscillation processes. The initial rise component is triggered by dipole-allowed charge transfer transition (from O 2p to Fe 3d). The fast-relaxation component corresponds to the electron-phonon thermalization. Extracted by a bi-exponential decay function, the electron-phonon thermalization time constant has been found to be sensitive to the structure of the BFO film sample.²³ Sheu *et al.* analyzed the subsequent slow relaxation with different optical excitation energies and found that the photo-excited electrons primarily leave the conduction band via radiative recombination.²⁴ Here, we concentrate on the appearance of the periodic oscillations during the slow-relaxation process. After deducting the background of the electron relaxation, the oscillation component can be obtained, which is plotted in Figures 2(a)–2(c). The fast Fourier transform (FFT) of the oscillations represents peaks around 36 GHz, 33 GHz, and 25 GHz for BLFNO films on (001)-Si, (001)-YSZ, and (001)-STO substrates, respectively, as shown in Figures 2(d)–2(f), which correspond to the LA phonon modes.²⁵ The oscillation frequency remains unchanged with increasing pump fluence, while the amplitude of the oscillation is proportional to the pump fluence. For these thin film samples, we do not identify the transverse acoustic (TA) phonons, which has been observed on [010] direction for rhombohedral symmetry of BFO single crystal.²⁵ The transient reflectivity changes without the relaxation background can be fitted by a damped harmonic function

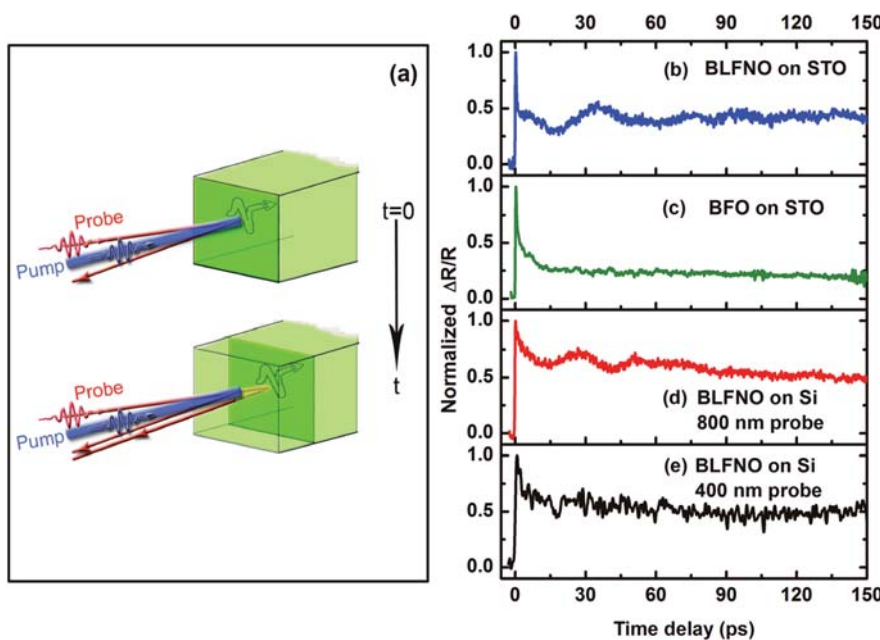


FIG. 1. (a) Schematic of the pump-probe experimental setup and the propagating strain wave model. Normalized transient reflectance changes $\Delta R/R$ of (b) BLFNO film and (c) BFO film on (001)-STO. Normalized transient reflectance changes $\Delta R/R$ of BLFNO film on (001)-Si probed with (d) 800 nm and (e) 400 nm at room temperature.

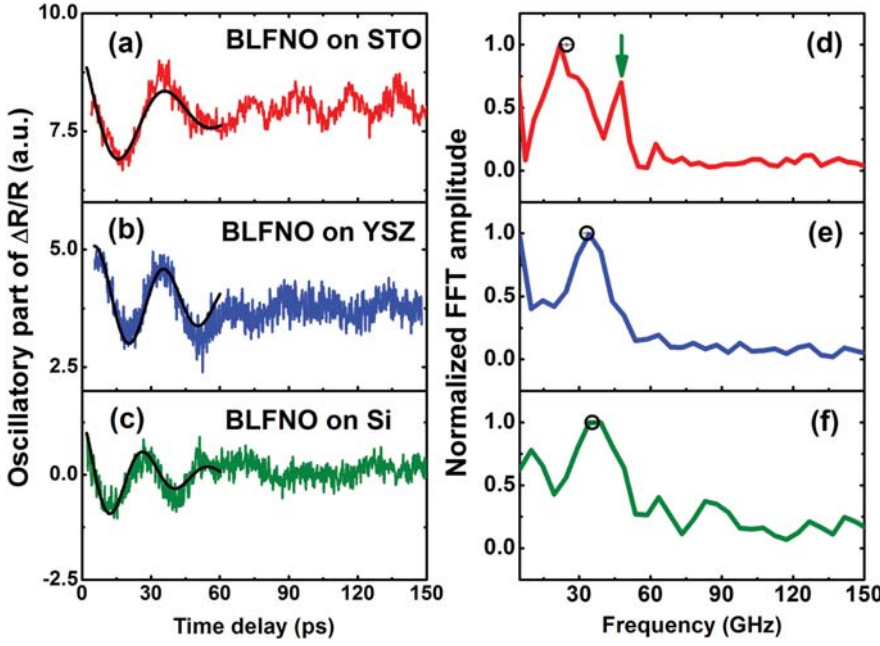


FIG. 2. (a)-(c) The oscillatory part of $\Delta R/R$ of BLFNO on various substrates, (001)-STO, (001)-YSZ, and (001)-Si, respectively. (d)-(f) The fast Fourier transform spectra obtained from $\Delta R/R$ without the relaxation background at room temperature. The solid lines and open circles in the figures are the fitting results by Eq. (2). The arrow at 47 GHz is assigned to LA phonon mode in the STO substrate.

$$\frac{\Delta R(t)}{R} \propto \cos(2\pi\Omega t - \phi)e^{-t/\tau}, \quad (2)$$

where Ω and τ are the oscillation frequency and the dephasing time, respectively. The black solid lines in Figures 2(a)–2(c) are simple-damped cosine fits, Ω of BLFNO films on (001)-Si, (001)-YSZ, and (001)-STO can be extracted as 35.5 ± 0.5 GHz, 33.3 ± 0.3 GHz, and 24.8 ± 0.2 GHz, respectively, as shown by the open circles in Figures 2(d)–2(f).

As the wave-vector conservation in back-scattered configuration, the wave-vector of the acoustic wave $q = 2k_{probe}$, where k_{probe} is the wave-vector of the probe beam with $k_{probe} = \frac{2\pi\sqrt{n^2 - \sin^2\theta}}{\lambda_{probe}}$, where n , θ , λ_{probe} are the refractive index of BLFNO films at probe beam wavelength, the incidence angle of the probe beam, and the wavelength of the probe beam, respectively. According to the strain pulse propagation model,^{25–28} the phonon dispersion is $2\pi\Omega = v_{Sound}q$. Thus, the sound velocity in the sample is given by

$$v_{Sound} = \Omega\lambda_{probe}/2\sqrt{n^2 - \sin^2(\theta)} \quad (3)$$

In our case, the θ approaches to 0° , the sound velocity can be reduced to $v_{Sound} = \Omega\lambda_{probe}/2n$. Consequently, the Brillouin frequency Ω is proportional to n/λ_{probe} .^{29,30} However, in our case, Figure 1(e) shows that no significant oscillation component of BLFNO film on (001)-Si is observed with probe wavelength of 400 nm beam. As Figure 1(a) sketched, the oscillation component of $\Delta R/R$ is ascribed to the interference between the probe beams reflected from the surface and the strain layer of the propagating strain pulse. The constructive or destructive interference depends not only on the position of the lattice modulation but also on the penetration depth of the probe beam ($\xi = \lambda_{probe}/4\pi\kappa$). ξ of BFO film at 400 nm probe beam (~ 40 nm) is much shorter than that at 800 nm probe beam ($\sim 10 \mu\text{m}$).^{8,24} This is the reason that the oscillations cannot be observed with 400 nm probe beam. In this study, we choose the wavelength of the probe beam at 800 nm, which is

allowed to investigate the elasticity deeply beneath the free surface. It should be mentioned that ξ at 800 nm is much larger than the thickness of BLFNO film. Therefore, it can be predicted that the strain wave will propagate from the BLFNO film into the substrate. As shown in Figure 2(d), the fast Fourier transform of the oscillations of the BLFNO on (001)-STO (Figure 2(a)) reveals two frequencies: ~ 25 and ~ 47 GHz, which are assigned to LA phonon modes in the BLFNO film and the STO substrate, respectively.²⁹ In addition, τ arises from two sources, the intrinsic lifetime of LA phonons (τ_{LA}) and the penetration depth of the probe light into the sample. τ can be expressed as a superposition, $\tau^{-1} = \tau_{LA}^{-1} + \tau_{\xi}^{-1}/V_{Sound}$. Due to the thickness of the thin film is much shorter than ξ , it is impossible to use the oscillation signal to evaluate the intrinsic lifetime of LA phonons in our case.

Photo-induced strain wave can have different generation mechanisms in different materials. For example, instantaneous thermal strain by pulsed lasers in opaque samples,^{26,28} impulsive stimulated Raman scattering in semiconductor superlattices,³¹ displacive excitation in bulk semiconductors,³² and ultrafast dynamical screening of the built-in piezoelectric field in quantum wells.³³ In order to elucidate the origin of the coherent acoustic phonon in BLFNO films, we choose the pure BFO thin films for comparison. As shown in Figure 1(c), the oscillation magnitude of $\Delta R/R$ is too weak to be identified clearly from the relaxation background in a pure BFO film on (001)-STO, which indicates that the LA phonon generation efficiency of BFO film can be efficiently enhanced through La and Nb codoped. Similar cases are also observed in the film samples on the other two substrates. La and Nb codoped BFO film has been proved to show better ferroelectric properties in terms of large polarization and significantly reduced electrical leakage.^{20,34} It is important to remind that the nonlinear susceptibility ($\chi^{(2)}$) is a function of ferroelectric polarization.²² Therefore, our finding suggests that the generation of acoustic phonons is strongly related to the optical rectification performance. The larger $P_0^{(2)}(t)$ can enhance the photo-induced strain wave via electrostriction

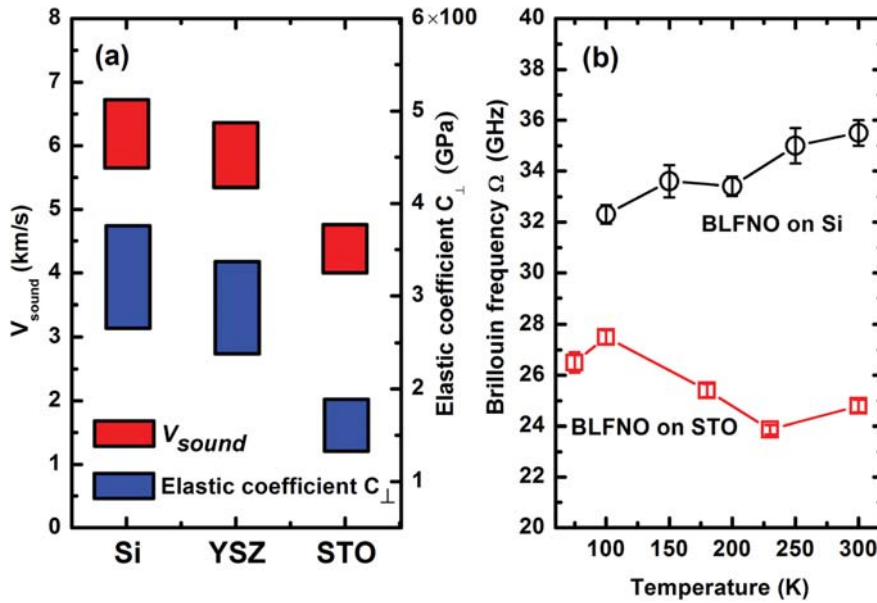


FIG. 3. (a) The estimated sound velocities of BLFNO on various substrates, (001)-STO, (001)-YSZ, and (001)-Si, respectively, as determined from the Brillouin frequencies and published values of refractive index n from 2.1 to 2.5. (b) Brillouin frequencies of BLFNO films on (001)-STO (squares) and (001)-Si (circles) as a function of temperature, respectively.

effect. Thus, our experimental observation can be used to verify the mechanism of the ultrafast optical-mechanical transferring in BFO films, the transient photostriction effect, a combination of the optical rectification effect, and electrostriction effect. It should be mentioned that, although light irradiation will cause subtle changes of the ferroelectric polarization under certain wavelength, the transient photostriction effect driven by the optical rectification effect with femtosecond laser pulse does not show any detectable changes after several measurements.

In general, the various elastic parameters are considered as the origin of many unexpected properties in BFO, such as the decrease of Curie temperature with strain,³⁵ the giant polarization and enhanced electromechanical response,³⁶ and a concurrent magnetic and ferroelectric transition at near room temperature of the tetragonal BFO.³⁷ The transient photostriction effect offers an available way to quantify the effect from substrate via the out-of-plane longitudinal elastic constant, C_{\perp} . Assuming the refractive index of doped BFO film ranged from $n = 2.1$ to $n = 2.5$,^{8,9,38} according to Eq. (3), we can estimate the sound velocities of the BLFNO films on different substrates, $v_{\text{sound}} = 4761\text{--}4000\text{ ms}^{-1}$ on (001)-STO, $v_{\text{sound}} = 6361\text{--}5344\text{ ms}^{-1}$ on (001)-YSZ, and $v_{\text{sound}} = 6723\text{--}5648\text{ ms}^{-1}$ on (001)-Si, which are summarized in Figure 3(a). C_{\perp} is determined from the longitudinal sound velocity and the mass density, ρ , by the relation $\rho(v_{\text{sound}})^2 = C_{\perp}$.²⁵ Using the mass density $\rho_{\text{BFO}} = 8340\text{ kg m}^{-3}$, the magnitudes of C_{\perp} of BLFNO films on different substrates can be estimated. Although arising from the refractive index evaluation, the uncertainties of the order of 40%, C_{\perp} still shows obvious substrate dependent, $C_{\perp} = 189\text{--}133\text{ GPa}$ on (001)-STO, $337\text{--}238\text{ GPa}$ on (001)-YSZ, and $376\text{--}266\text{ GPa}$ on (001)-Si, as shown in Figure 3(a). It can be found that the polycrystalline BLFNO films grown on (001)-Si and (001)-YSZ have the similar value of C_{\perp} , while the longitudinal elastic constant is much reduced in the epitaxially grown BLFNO film on (001)-STO substrate. Furthermore, the temperature dependences of Ω of the BLNFO films on (001)-STO and (001)-Si substrates are shown in Figure 3(b), respectively. It is seen that Ω of the

BLNFO film on (001)-Si changes less than 10%, from $35.5 \pm 0.5\text{ GHz}$ to $32.3 \pm 0.4\text{ GHz}$, when temperature decreases from 300 K to 70 K, which indicates that LA phonon mode shows weak temperature dependence. In contrast, LA phonon mode of the epitaxially grown BLFNO film on (001)-STO is almost no temperature dependence. Our BLFNO film epitaxially grown on (001)-STO substrate has a tetragonal structure in comparison to the rhombohedral structure of the polycrystalline film on YSZ and Si substrates. These experimental results quantitatively indicate that the propagation of LA phonons in BLFNO films is strongly modified by the strain from substrate.

In conclusion, pump-probe spectroscopy with short-pulsed laser can be used to study the transient photostriction effect in multiferroic BLFNO thin films via the generation and propagation of the GHz coherent acoustic phonons. The substrate- and temperature-dependence of the propagation of LA phonons not only provide the out-of-plane elastic modulus of BLFNO films but also give the insight on the dynamical coupling between polarization and lattice deformation. It is also demonstrated that the transient photostriction can be designed and monitored by doping and strain engineering in BFO thin films. As far as applications are concerned, the ultrafast coupling of light with mechanical degrees of freedom guides the promising practical applications in types of photo-driven remote control BFO-based wireless device, sensor, and other optomechanical micro/nano systems.

The research was supported by National Natural Science Foundation of China (Grant No. 11174195). Z. X. Cheng thanks Australia Research Council for support through a Future Fellowship (FT 0990287).

¹W. Eerenstein, N. D. Mathur, and J. F. Scott, *Nature* **442**, 759 (2006).

²S. W. Cheong and M. Mostovoy, *Nature* **6**, 13 (2007).

³K. F. Wang, J.-M. Liu, and Z. F. Ren, *Adv. Phys.* **58**, 321(2009).

⁴T. Kimura, T. Goto, H. Shintani, K. Ishizaka, T. Arima, and Y. Tokura, *Nature* **426**, 55 (2003).

⁵Z. Cheng and X. Wang, *Phys. Rev. B* **75**, 172406 (2007).

⁶B. Ramachandran, A. Dixit, R. Naik, G. Lawes, and M. S. Ramachandra Rao, *Phys. Rev. B* **82**, 012102 (2010).

- ⁷R. V. Pisarev, A. S. Moskvin, A. M. Kalashnikova, and Th. Rasing, *Phys. Rev. B* **79**, 235128 (2009).
- ⁸A. Kumar, R. C. Rai, N. J. Podraza, S. Denev, M. Ramirez, Y.-H. Chu, L. W. Martin, J. Ihlefeld, T. Heeg, J. Schubert, D. G. Schlom, J. Orenstein, R. Ramesh, R. W. Collins, J. L. Musfeldt, and V. Gopalan, *Appl. Phys. Lett.* **92**, 121915 (2008).
- ⁹B. Gu, Y. Wang, J. Wang, and W. Ji, *Opt. Express* **17**, 10970 (2009).
- ¹⁰J. Kreisel, M. Alexe, and P. A. Thomas, *Nature Mater.* **11**, 260 (2012).
- ¹¹S. R. Basu, L. W. Martin, Y. H. Chu, M. Gajek, R. Ramesh, R. C. Rai, X. Xu, and J. L. Musfeldt, *Appl. Phys. Lett.* **92**, 091905 (2008).
- ¹²T. Choi, S. Lee, Y. J. Choi, V. Kiryukhin, and S.-W. Cheong, *Science* **324**, 63 (2009).
- ¹³H. T. Yi, T. Choi, S. G. Choi, Y. S. Oh, and S.-W. Cheong, *Adv. Mater.* **23**, 3403 (2011).
- ¹⁴B. Kundys, M. Viret, D. Colson, and D. O. Kundys, *Nature Mater.* **9**, 803 (2010).
- ¹⁵B. Kundys, M. Viret, C. Meny, V. Da Costa, D. Colson, and B. Doudin, *Phys. Rev. B* **85**, 092301 (2012).
- ¹⁶D. S. Rana, I. Kawayama, K. Mavani, K. Takahashi, H. Murakami, and M. Tonouchi, *Adv. Mater.* **21**, 2881 (2009).
- ¹⁷D. Talbayev, S. A. Trugman, S. Lee, H. T. Yi, S.-W. Cheong, and A. J. Taylor, *Phys. Rev. B* **83**, 094403 (2011).
- ¹⁸Z. X. Cheng, A. H. Li, X. L. Wang, S. X. Dou, K. Ozawa, H. Kimura, S. J. Zhang, and T. R. Shroud, *J. Appl. Phys.* **103**, 07E507 (2008).
- ¹⁹R. D. Averitt and A. J. Taylor, *J. Phys.: Condens. Matter* **14**, R1357 (2002).
- ²⁰Z. Cheng, X. Wang, S. Dou, H. Kimura, and D. Ozawa, *Phys. Rev. B* **77**, 092101 (2008).
- ²¹Y. R. Shen, *The Principles of Nonlinear Optics* (Wiley, New York, 1984).
- ²²L. Y. Chen, J. C. Yang, C. W. Luo, C. W. Laing, K. H. Wu, J.-Y. Lin, T. M. Uen, J. Y. Juang, Y. H. Chu, and T. Kobayashi, *Appl. Phys. Lett.* **101**, 041902 (2012).
- ²³Z. Jin, Y. Xu, Z. Zhang, G. Li, X. Lin, G. Ma, Z. Cheng, and X. Wang, *Appl. Phys. Lett.* **100**, 071105 (2012).
- ²⁴Y. M. Sheu, S. A. Trugman, Y.-S. Park, S. Lee, H. T. Yi, S.-W. Cheong, Q. X. Jia, A. J. Taylor, and R. P. Prasankumar, *Appl. Phys. Lett.* **100**, 242904 (2012).
- ²⁵P. Ruello, T. Pezeril, S. Avanesyan, G. Vaudel, V. Gusev, I. C. Infante, and B. Dkhil, *Appl. Phys. Lett.* **100**, 212906 (2012).
- ²⁶C. Thomsen, H. T. Grahn, H. J. Maris, and J. Tauc, *Phys. Rev. B* **34**, 4129 (1986).
- ²⁷I. Bozovic, M. Schneider, Y. Xu, R. Sobolewski, Y. H. Ren, G. Lüpke, J. Demsar, A. J. Taylor, and M. Onellion, *Phys. Rev. B* **69**, 132503 (2004).
- ²⁸C. Thomsen, H. T. Grahn, H. J. Maris, and J. Tauc, *Opt. Commun.* **60**, 55 (1986).
- ²⁹Y. H. Ren, M. Trigo, R. Merlin, Venimadhav Adyam, and Qi Li, *Appl. Phys. Lett.* **90**, 251918 (2007).
- ³⁰H. C. Shih, L. Y. Chen, C. W. Luo, K. H. Wu, J.-Y. Lin, J. Y. Juang, T. M. Uen, J. M. Lee, J. M. Chen and T. Kobayashi, *New J. Phys.* **13**, 053003 (2011).
- ³¹A. Bartels, T. Dekorsy, H. Kurz, and K. Köhler, *Phys. Rev. Lett.* **82**, 1044 (1999).
- ³²M. D. Cummings and A. Y. Elezzabi, *Appl. Phys. Lett.* **79**, 770 (2001).
- ³³P. J. S. van Capel, D. Turchinovich, H. P. Porte, S. Lahmann, U. Rossow, A. Hangleiter, and J. I. Dijkhuis, *Phys. Rev. B* **84**, 085317 (2011).
- ³⁴Y.-H. Lee, J.-M. Wu, and C.-H. Lai, *Appl. Phys. Lett.* **88**, 042903 (2006).
- ³⁵St. Kovachev and J. M. Wesselinowa, *J. Phys.: Condens. Matter* **21**, 395901 (2009).
- ³⁶R. J. Zeches, M. D. Rossell, J. X. Zhang, A. J. Hatt, Q. He, C.-H. Yang, A. Kumar, C. H. Wang, A. Melville, C. Adamo, G. Sheng, Y.-H. Chu, J. F. Ihlefeld, R. Erni, C. Ederer, V. Gopalan, L. Q. Chen, D. G. Schlom, N. A. Spaldin, L. W. Martin, and R. Ramesh, *Science* **326**, 977 (2009).
- ³⁷K.-T. Ko, M. H. Jung, Q. He, J. H. Lee, C. S. Woo, K. Chu, J. Seidel, B.-G. Jeon, Y. S. Oh, K. H. Kim, W.-I. Liang, H.-J. Chen, Y.-H. Chu, Y. H. Jeong, R. Ramesh, J.-H. Park, and C.-H. Yang, *Nat. Commun.* **2**, 567 (2011).
- ³⁸A. Gaur, P. Singh, N. Choudhary, D. Kumar, M. Shariq, K. Singh, N. Kaur, and D. Kaur, *Physica B* **406**, 1877 (2011).